



Low Temperature Cure Siloxane Based Hybrid Renewable Cardanol Benzoxazine Composites for Coating Applications

V. Selvaraj¹ · T. R. Raghavarshini¹ · M. Alagar²

© Springer Science+Business Media, LLC, part of Springer Nature 2019

Abstract

The siloxane based flexible cardanol benzoxazine was synthesised using cardanol, 1,3-bis(aminopropyl) tetramethyldisiloxane and *p*-formaldehyde through solvent free method and was characterised by different analytical techniques. A new fangled nanocomposites of amine functionalised rice husk ash silica reinforced siloxane based flexible cardanol benzoxazine were developed and their molecular structure, molecular weight, morphology, cure behaviour, thermal stability, dielectric character and corrosion resistant behaviour were carried out by appropriate test methods. Data obtained from differential calorimetric analysis and experimental cure process infer that the siloxane based cardanol benzoxazine cures at 110 °C, which is significantly lower temperature when compared to that of conventional benzoxazines cure between 220 and 280 °C. Results from dielectric and corrosion resistant studies indicate that these renewable hybrid composite materials can be conveniently used in the form of adhesives, encapsulants, sealants and potting compounds for high performance, low k materials in microelectronics and as coatings to protect steel surfaces from corrosion and microbial deterioration.

Keywords Siloxane based cardanol-benzoxazine · Amine functionalized rice husk ash silica · Hybrid bio-nanocomposites · Low temperature cure · Low k dielectric · Corrosion resistance

Introduction

The petrochemical based phenolic compounds are used for the synthesis of benzoxazines via a Mannich-condensation process [1–3]. These phenolic compounds possess an advanced characteristic properties like low water absorption, high thermal stability with high mechanical strength [4–6]. Benzoxazines also have certain drawbacks like high curing temperature and brittle behaviour of the cured matrices. To overcome these drawbacks, researchers around the world are making sustained efforts to utilize the renewable plant oil based phenolic compounds for the synthesis of benzoxazines instead of petroleum based raw materials [7–12]. In

this connection, cashew nut shell liquid (CNSL) based raw materials are considered as most versatile due to their significant properties and competitive cost. The benzoxazines synthesized from cashew nut shell liquid (CNSL) are used for a number of applications in the form of coatings, sealants, adhesives and matrices for different industrial applications [13–21]. In addition, benzoxazines derived from cardanol can be used as potential corrosion resistant materials to protect mild steel specimens from corrosion [22–28]. Furthermore, natural rice husk silica (SiO₂) obtained through the calcination process of rice husk has been used to remove the bacteria and microbes in water [29]. In the present work, bio-silica obtained from rice husk ash functionalized using aminosilane derivative has been reinforced with cardanol benzoxazine to improve corrosion protection in addition to low temperature cure behaviour and enhanced thermal properties [30–37].

The modern surface coating industries need a high performance organic resin binder, which is able to hold other additives viz., fillers, colourants, plasticizers, extenders and functional additives, etc., uniformly and homogeneously in the coating system. Since, benzoxazine resins of the modified phenolic materials received considerable importance

✉ V. Selvaraj
rajselva_77@yahoo.co.in; vaithilingamselvaraj@gmail.com

¹ Nanotech Research Lab, Department of Chemistry, University College of Engineering Villupuram (A Constituent College of Anna University, Chennai), Kakuppam, Villupuram, Tamil Nadu 605 103, India

² Polymer Engineering Laboratory, PSG Institute of Technology and Applied Research, Coimbatore, Tamil Nadu 641 062, India

in the resin industries due their high performance characteristics, i.e. high thermal stability, improved dielectric and surface properties, cures in the absence of catalyst and competitive cost. Though, the benzoxazines possess a number of advantages, it has some of the short comings like high cure temperature and brittle behaviour of cured matrix. Researchers around the world are continuously making efforts to alleviate these problems and to utilize the benzoxazine based materials in the form of high performance coatings, matrices and composites for advanced applications [38, 39]. In detail, the cardanol derived from cashew nut shell liquid was used for the synthesis of a novel siloxane based cardanol-benzoxazine by reacting cardanol with 1,3-bis (aminopropyl) tetramethyl disiloxane as amine component and paraformaldehyde through solvent free method. In addition, biobased phenolic compound was also used along with biobased silica (husk ash silica) and the prepared composites also cured in the same temperature, which was also expected to enhance the performance of the coating material in microelectronic applications. The prime objective of the present study is to reduce the curing temperature of the benzoxazine prepared using cardanol as bio-resource material to extent possible preferably below 150 °C without compromising the existing properties of the materials. Further, if the temperature was reduced to room temperature, then bio-based benzoxazine can be used in the paint industry and other various applications at ambient temperature. With this in mind, the present work was carried out to develop benzoxazine using sustainable bio-resource material cardanol, with a view to impart flexibility of the resulting benzoxazine and a siloxane component to lowers the curing temperature in addition to contribution of toughness and flexibility. As expected, the resulted siloxane modified benzoxazine possesses a surprisingly low cure temperature (110 °C) when compared to that of conventional benzoxazines (220–280 °C). In addition to that the further processes to reduce the curing temperature are also under progress using natural resources. Additionally, the siloxane modified benzoxazine was reinforced with varying weight percentages of bio-silica obtained from rice-husk to obtain hybrid composites with enhanced thermal stability, low dielectric behaviour and better surface properties. The physicochemical, thermal, morphology, dielectric and corrosion resistant behaviour of cardanol-benzoxazine composites have been studied using appropriate analytical test methods and the data resulted are discussed and reported. Results obtained from different analysis and experiments, it is suggested that these siloxane modified benzoxazine can be used as better hybrid resinous material for coatings and sealants for efficient microelectronics insulation applications.

Experimental Materials

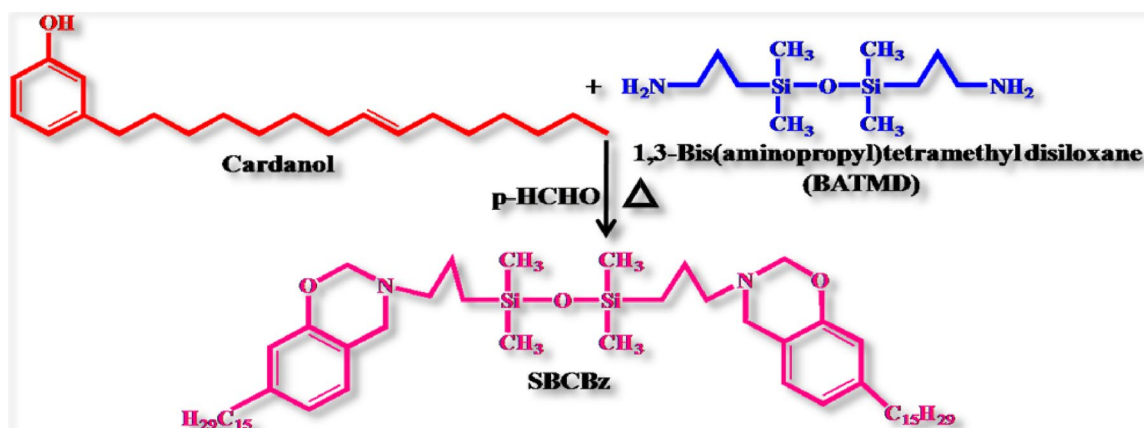
The cardanol was obtained from Satya Cashew Chemicals Pvt. Ltd. Chennai, (India). Ethanol and dichloromethane were purchased from Merck. Hydrochloric acid (99%) and chloroform were purchased from Fisher scientific. Para formaldehyde, sodium hydroxide, sodium sulphate, 3-Aminopropyltrimethoxysilane (APTMS) and dichlorodimethylsilane were obtained from Sigma Aldrich. 1,3-bis(aminopropyl)tetramethyl disiloxane were procured from Alfa Aesar. Rice husk was obtained from the local rice mill, Pathirakottai, Cuddalore district, Tamil Nadu, India.

Synthesis of 1,3-Bis(aminopropyl)tetramethyl Disiloxane Based Cardanol Benzoxazine Monomer

The synthesis of siloxane based cardanol benzoxazine was carried out using natural cardanol oil, paraformaldehyde and 1,3-bis(aminopropyl)tetramethyl disiloxane [40]. Typically, 3.5 g of 1,3-bis(aminopropyl)tetramethyl disiloxane was stirred with 1 g of *p*-formaldehyde for 1 h at 85 °C. 5 g of cardanol was added to the above reaction mixture and the temperature was slowly reduced to 50 °C. The reaction was continued for another 10 h and the completion of the reaction was monitored and confirmed by Thin Layer Chromatography (TLC) analysis. Then, the resulted reaction product was poured into 2 N sodium hydroxide solution and the product benzoxazine was extracted with chloroform. The obtained organic layer was washed with distilled water and the separated organic layer was dried over the anhydrous sodium sulphate and filtered. The solvent was removed under reduced pressure in order to obtain a red coloured siloxane diamine based cardanol benzoxazine (SBCBz) monomer (Scheme 1).

Preparation of Rice Husk Ash Silica and Amine Functionalized Rice Husk Ash Silica

Rice husk ash silica was prepared as per the previous reported method [41]. Rice husk obtained from the local rice mill was washed with double distilled water for several times and then dried in the sunlight for a week. The sunlight dried rice husk was burned in open air and crushed to obtain rice husk ash and collected. 50 g of crushed rice husk ash was immersed in one litre of 1 M HCl solution for 12 h and washed with double distilled water until the solution turn into neutral. The wet rice husk ash was dried in an oven at 100 °C for 48 h. The dried rice husk ash was taken in a silica crucible and placed in the muffle furnace



Scheme 1 Synthesis of 1,3-bis(aminopropyl)tetramethyl disiloxane based cardanol benzoxazine monomer

at 350 °C for 3 h and 600 °C for 6 h. The resulted white rice husk ash silica (RHAS) was stored for further process.

Synthesis of Amine Functionalized Rice Husk Ash Silica (ARHAS) from Rice Husk Ash

A tailored method was used for the preparation of amine functionalized rice husk ash silica [42–45]. For the preparation of amine functionalized rice husk ash, 10 g of rice husk ash silica was dispersed in 80 mL of toluene for 2 h under nitrogen atmosphere in a 250 mL round bottomed flask. 4 mL of APTMS was added in drop wise to the above reaction mixture. After the addition of APTMS to the rice husk ash silica, the solution was ultrasonicated for 30 min. Then, the reaction mixture was refluxed under a nitrogen atmosphere at 80 °C for 24 h. The resulted product was filtered, washed with ethanol and dichloromethane and then dried in an oven at 70 °C for 24 h. Finally, the prepared amine functionalized rice husk ash silica (Scheme 2) was characterised and used as reinforcement for the preparation of cardanol based benzoxazine nanocomposites.

Preparation of Amine Functionalized Rice Husk Ash Silica Reinforced Siloxane Based Cardanol-Benzoxazine (ARHAS/SBPCBz) Composites

The amine functionalized rice husk ash silica reinforced siloxane based cardanol-benzoxazine (ARHAS/SBPCBz) composites are prepared as per the Scheme 3. Typically, the varying weight percentages (0 wt%, 1 wt%, 3 wt% and 5 wt%) of amine functionalized rice husk ash silica (ARHAS) was separately dispersed in 5 mL chloroform. 2 g of cardanol based benzoxazine monomer was dispersed in 10 mL chloroform and gradually added to the above ARHAS dispersions and stirred continuously for 24 h. Then, the solutions were poured into respective dichlorodimethylsilane coated

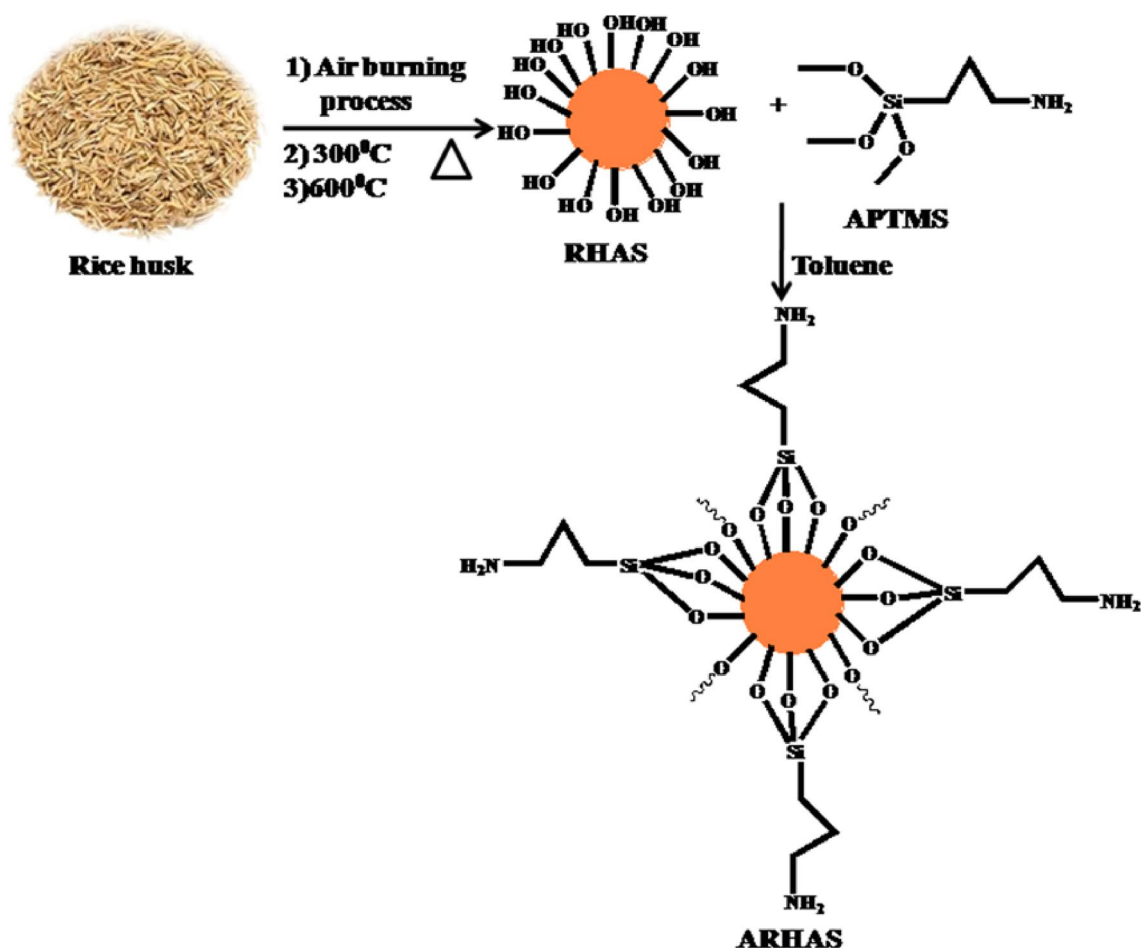
glass plates and cured at 30 °C, 50 °C, 70 °C, 90 °C for 1 h at each temperature and then 110 °C for 5 h to obtain a smooth flexible thin film of cardanol-benzoxazine composites (Scheme 3).

Testing of the Prepared Sample in Seawater for Marine Applications

The low temperature cured flexible siloxane based cardanol benzoxazine and its composite films reinforced with different weight percentages of ARHAS are placed in the natural sea water for seven months and their surface changes were checked using microscopy at different intervals of time [46]. At the end of every time interval, the test sample, i.e., the soaked cardanol based benzoxazine matrix and its composites have been taken out, wiped using tissue paper and then dried for a few minutes to evaporate moisture and then placed in the microscope to capture the surface change as the photo images. After that the captured hybrid samples were again soaked in the sea water and this process was repeated for different intervals of time. For each case, three samples per experiment were carried out. Moreover, to check the reproducibility for each stage, the fresh samples were also used for each period of experiments along with the used samples. The composition of natural sea water collected from East-Coast of Bay of Bengal, Cuddalore was analysed with the help of KBS Industry, Kalaingar Karunanithi Street, Gingee Road, Villupuram, Tamil Nadu, India and the results obtained are presented in Table 1.

Electrochemical Studies

The corrosion resistant behaviour of cardanol-benzoxazine matrix and composite samples were studied using two electrode systems to get Nyquist and Tafel plots. For corrosion



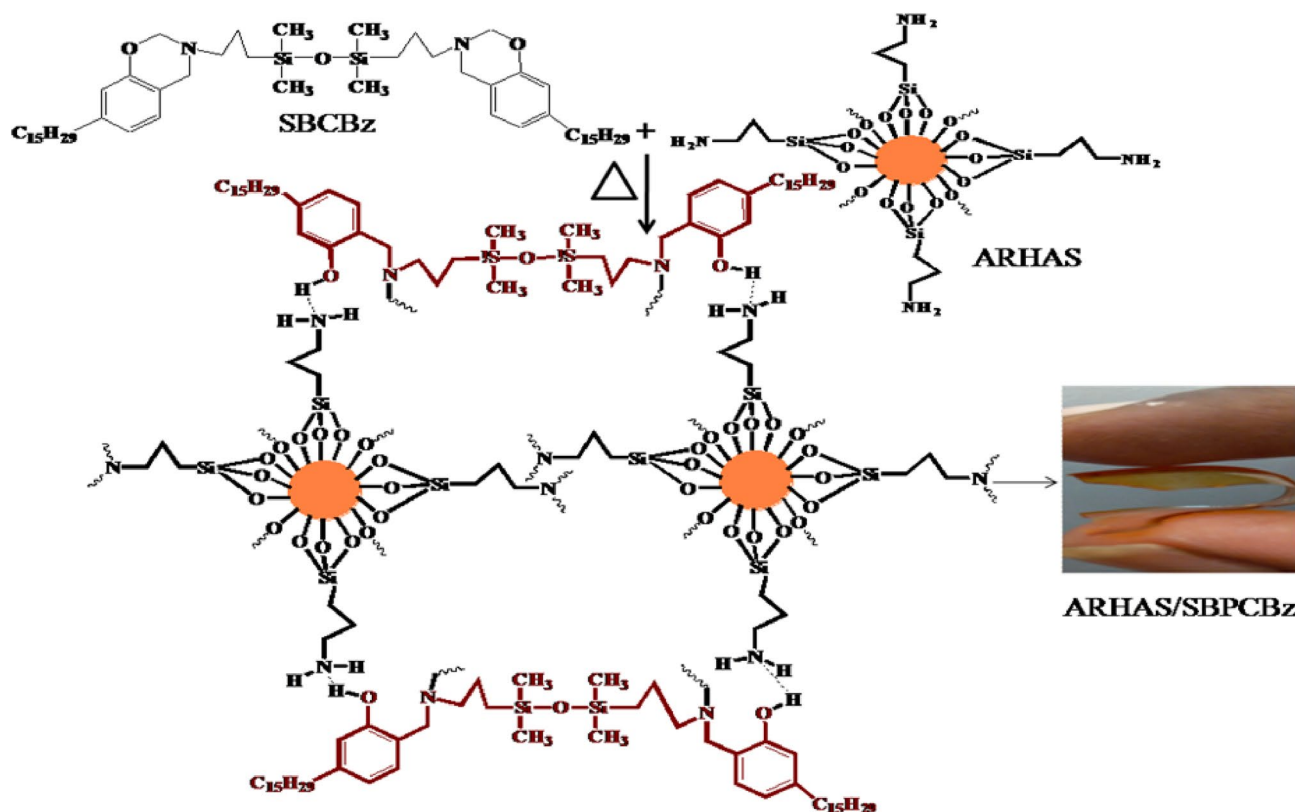
Scheme 2 Preparation of amine functionalized rice husk ash silica (ARHAS) using APTMS and RHAS

experiment, the mild steel plate was cut into $5\text{ cm} \times 1\text{ cm}$ and then the samples were coated on the mild steel plate with the area as $1 \times 1\text{ cm}$. The coated mild steel plates were soaked for 1 h in synthetic sea water (3.5 wt% NaCl solution), which is then used as working electrode and Ag/AgCl used as a reference electrode.

Characterization

Fourier Transform Infra Red Spectra were obtained from Perkin Elmer spectrometer with KBr disc for rice husk ash silica and ARHAS while without KBr disc for siloxane based cardanol-benzoxazine and its composites. ^1H NMR and ^{13}C NMR spectra were carried out on a 400 MHz Bruker EXT40617 spectrometer at $25\text{ }^\circ\text{C}$ using CDCl_3 as solvent. X-ray diffraction analysis was carried out at ambient temperature using a Rich Seifert (Model 3000) with the diffraction angle at 2θ from 0° to 80° . The morphological images were obtained from using scanning electron microscope of JEOL JSM-5610LV. The transmission electron

microscopy (TEM) analysis of hybrid benzoxazine composites was carried out using the TEM model Joel/JEM 2100 with the source of LaB6. The resolution point of the TEM is 0.23 nm and the lattice is 0.14 nm with the accelerating voltage of 200 kV. Dielectric studies were carried out in a frequency range of 10 Hz–1 MHz using HIOKI 3532 50LCR HITESTER. Thermal Gravimetric analysis (TGA) was carried out using METTLER TOLEDO micro and ultra-micro balances with sub-microgram resolution at a temperature range up to $800\text{ }^\circ\text{C}$. Differential Scanning Calorimetry (DSC) analysis was carried out using DSC Q200V23.10 Build 79 models with the temperature range from 0 to $300\text{ }^\circ\text{C}$. GEMKOLABWELL Baby Microscope with $10\times$ OBJECTIVE, $\times 10\text{ E.P.}$, $\times 1000$ magnification of an eyepiece and H10 \times Light with reflecting mirror was used to determine the photo images of cardanol-benzoxazine and its composite films. The electrochemical impedance and Tafel plots were obtained using Biologic VSP2 multichannel (France) workstation analyzer in order to predict the anticorrosion properties.



Scheme 3 Amine functionalized rice husk ash silica reinforced siloxane based polycardanol benzoxazine composites (ARHAS/SBPCBz)

Table 1 The composition of natural sea water collected from East-Coast of Bay of Bengal, Cuddalore to ascertain the antifouling effect

S. no.	Parameter	Permissible unit of distilled water	Observed values of sea water
1.	Chloride	8.5	1150 mg/l
2.	Sulphate	200	1100 mg/l
3.	Alkalinity	200	1400 mg/l
4.	Magnesium	30	20.4 mg/l
5.	Calcium	75	46.5 mg/l
6.	pH	6.5	7.1
7.	Total dissolved solids	500	7920 ppm

Results and Discussion

Characteristic Studies of Siloxane Based Cardanol-Benzoxazine Monomer

Figure 1 shows the FTIR spectrum of siloxane based cardanol-benzoxazine monomer. The characteristic absorption bands obtained between 2927 cm^{-1} and 2853 cm^{-1} are indicating the presence of the alkyl side chain of the cardanol. The absorption peak for benzene ring has been

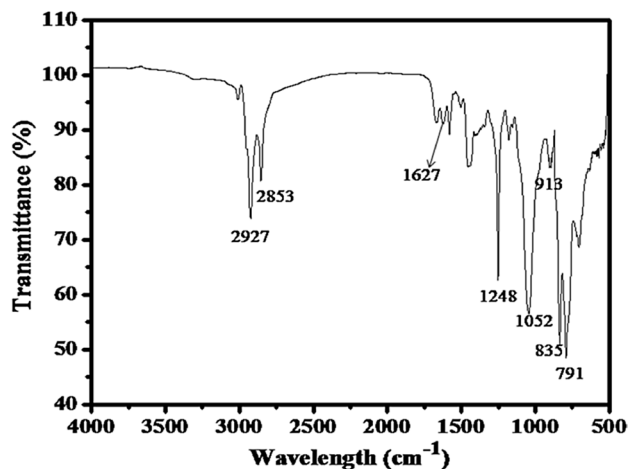


Fig. 1 FTIR spectrum of siloxane based cardanolbenzoxazine (SBCBz) monomer

visualised at 1627 cm^{-1} , which is due the stretching vibration of aromatic $\text{C}=\text{C}$ group [47]. The $\text{C}-\text{O}-\text{C}$ asymmetric and symmetric stretching vibrations of the oxazine ring were noticed at 1052 cm^{-1} and 1248 cm^{-1} , respectively [48]. The absorption peak appeared at 913 cm^{-1} infers the ring closure and formation of oxazine ring. The peaks

observed at 835 cm^{-1} and 791 cm^{-1} ascertain the presence of $-\text{Si}-\text{O}-\text{Si}-$ moieties of 1,3-bis(aminopropyl) tetramethyl disiloxane. Thus, the FTIR study confirms the formation of siloxane based cardanol-benzoxazine.

The ^1H NMR spectrum obtained for siloxane based cardanol-benzoxazine monomer is presented in Fig. 2. The peak (k) obtained at 3.6 ppm indicates the presence of $\text{Ph}-\text{CH}_2-\text{N}$ group and the peak appeared at 5.01 ppm (l) indicates the presence of $\text{O}-\text{CH}_2-\text{N}$ group, which confirms the formation of oxazine ring [49, 50]. The signals obtained between 6.51 and 6.90 ppm (n to p) infer the presence of aromatic protons attached to the oxazine ring structure. The peak appeared at 5.48 ppm (m) was assigned to $-\text{CH}=\text{CH}-$ protons present in the alkyl side chain of the cardanol structure [51]. The terminal methyl group from the cardanol side chain was appeared at 0.96 ppm (c) [52]. The peaks visible between 1.29 to 2.55 ppm (d to j) are indicating the $-\text{CH}_2-$ proton. The methyl proton of $-\text{Si}-\text{CH}_3$ group was observed at 0.08 ppm and 0.5 ppm for $-\text{CH}_2-\text{Si}-$ group present in 1,3-bis(aminopropyl)tetramethyl disiloxane [53]. Therefore, the NMR spectrum confirms the formation of siloxane based cardanolbenzoxazine monomer compound.

The ^{13}C NMR spectrum obtained for siloxane based cardanol-benzoxazine monomer is shown in Fig. 3. The signals observed at 82.8 ppm (n) and 57.5 ppm (m) indicate the carbon atoms of $-\text{O}-\text{CH}_2-\text{N}$ and aromatic- CH_2-N groups, respectively. These carbon signals are confirming the formation of oxazine ring. The peaks appeared at 138.2 ppm (t) and 130.7 ppm (s) infer the presence of aromatic carbon and $-\text{C}=\text{C}-$ carbon present in the aliphatic side chain of

the cardanol-benzoxazine monomer, respectively [54]. The methyl carbon of $\text{CH}_3-\text{Si}-$ and the terminal methyl carbon of CH_3-CH_2 are visible at 2.8 ppm (a) and 14.1 ppm (b), respectively. The chemical shifts observed between 22.8 and 36.3 ppm indicate the $-\text{CH}_2-$ carbon and the carbon signals obtained between 119.5 and 129.7 ppm represent the carbon atoms present in the aromatic ring.

The molecular weight of the monomer was confirmed by MALDI-TOF Mass spectroscopy (Fig. 4). From the MALDI mass spectrum, the molecular ion peak was observed at 900.7 (m/z) and the theoretically calculated molecular weight of the newly developed benzoxazine monomer sample is 902. Therefore, the molecular ion peak observed at 900.7 m/z (m^{-1}) in MALDI-TOF spectrum confirms the formation of the synthesised cardanol-benzoxazine monomer [55].

FTIR spectra (Fig. 5) provide the details about the absorption peaks of aminopropyl trimethoxysilane (APTMS), rice husk ash silica (RHAS) and amine functionalized rice husk ash silica (ARHAS). The broad absorption peak obtained from 3623 to 3456 cm^{-1} denotes the presence of the hydrogen bonded hydroxyl group and confirm the presence of $-\text{Si}-\text{OH}$ group in rice husk ash silica (RHAS). In the case of amine functionalized rice husk ash silica (ARHAS), the broad absorption peak appeared at 3339 cm^{-1} indicates the presence of $-\text{NH}_2$ group from APTMS [56, 57]. The absorption peaks appeared for RHAS and ARHAS at 1068 and 796 cm^{-1} ascertain the presence of $-\text{Si}-\text{O}-\text{Si}-$ linkages. The peak obtained at 1163 cm^{-1} infers the presence of $\text{Si}-\text{O}-\text{C}$ bond vibration [58]. Correspondingly, the absorption peaks

Fig. 2 ^1H NMR spectrum of siloxane based cardanolbenzoxazine (SBCBz) monomer

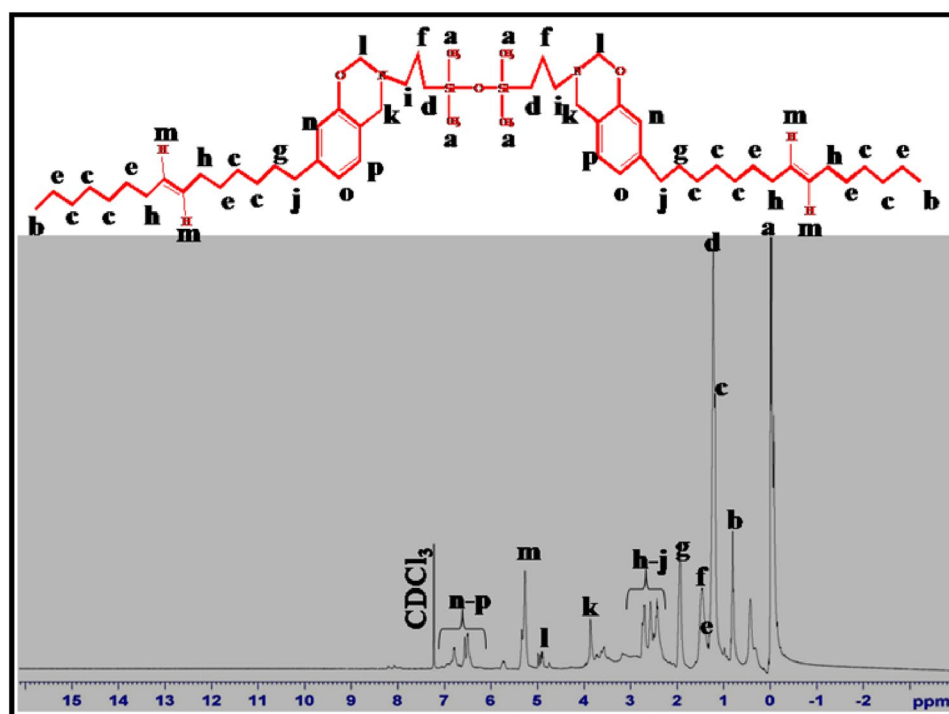


Fig. 3 ^{13}C NMR spectrum of siloxane based cardanol-benzoxazine (SBCBz) monomer

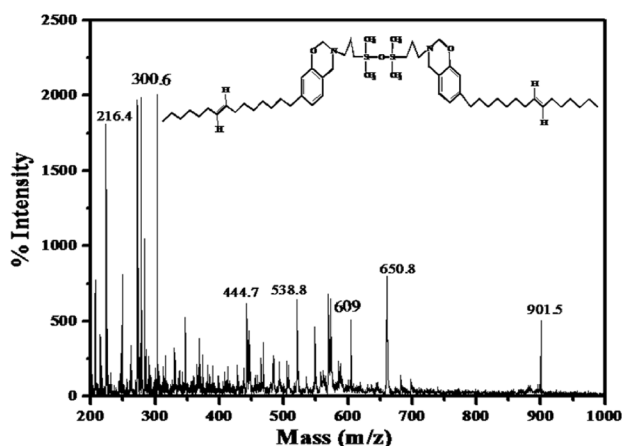
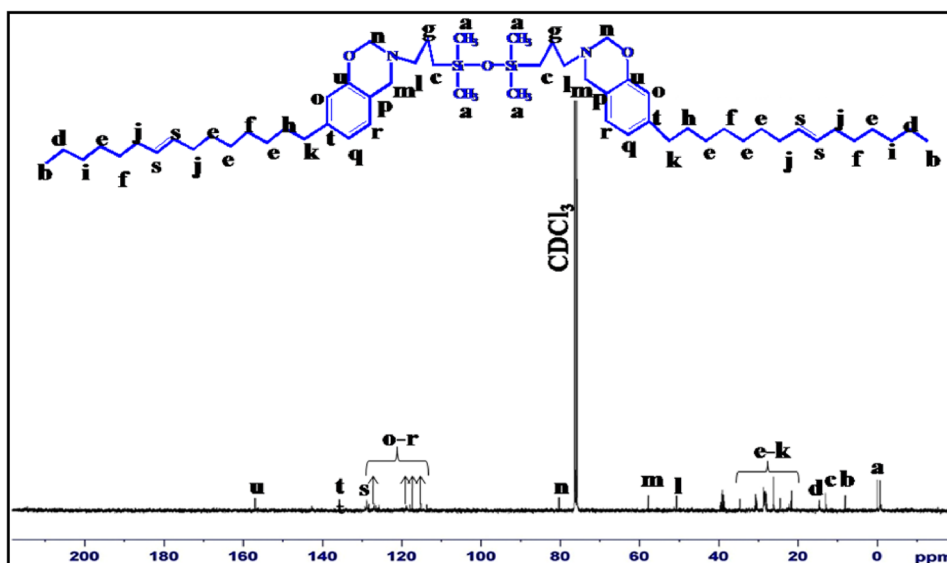


Fig. 4 MALDI-Mass spectrum of siloxane based cardanol benzoxazine monomer

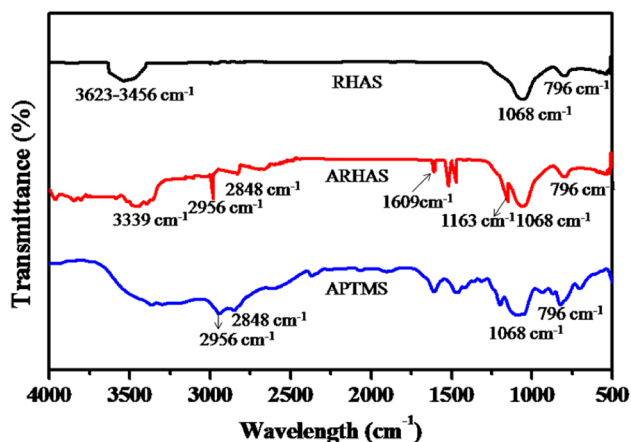


Fig. 5 FTIR spectra of aminopropyl trimethoxysilane, rice husk ash silica and amine functionalized rice husk ash silica compounds

observed at 2956 cm^{-1} and 2848 cm^{-1} infer the existence of $-\text{CH}_2$ stretching vibration. The bending vibration peak obtained at 1609 cm^{-1} confirms the presence of a primary amine group of $\text{N}-\text{H}$ from APTMS. The DSC analysis obtained for siloxane based monomeric cardanol-benzoxazine confirms that the newly developed benzoxazine cures at the range of 80 to $110\text{ }^\circ\text{C}$ (Fig. 10), which is the prime objective of the present work and this is considered to be a breakthrough in benzoxazine cure chemistry. This further enhances the utility of benzoxazine materials extending area of applications.

FTIR and Morphological Studies of SBPCBz Matrix and ARHAS/SBPCBz Composites

The FTIR studies of cured siloxane based cardanol-benzoxazine and its composites were carried out and the FTIR spectra were done with cured sample in the form of thin films without making pellets (Fig. 6a). The absorption peak obtained at 2834 cm^{-1} indicates the existence of intra-molecular hydrogen bonding of $-\text{O}\cdots\text{H}+\cdots\text{N}$ and the peaks obtained at 3352 cm^{-1} for neat SBPCBz and 3317 cm^{-1} for 1, 3 and 5 wt% of ARHAS/SBPCBz infer the presence of inter-molecular hydrogen bonding of $\text{OH}\cdots\text{O}$ in the molecule of neat SBPCBz, whereas the formation of both inter-molecular and intra-molecular hydrogen bonding also observed in the cases of varying weight percentages of ARHAS reinforced hybrid composites [59]. Hence, the inter-molecular and intra-molecular hydrogen bonding were taking place while curing of siloxane based cardanolbenzoxazine monomer to form polymer matrix and its composites, which in turn enhances the thermal behaviour to an appreciable extent. The absorption peak becomes visible at 2922 cm^{-1} represents the alkyl $-\text{CH}_2$ stretching group of

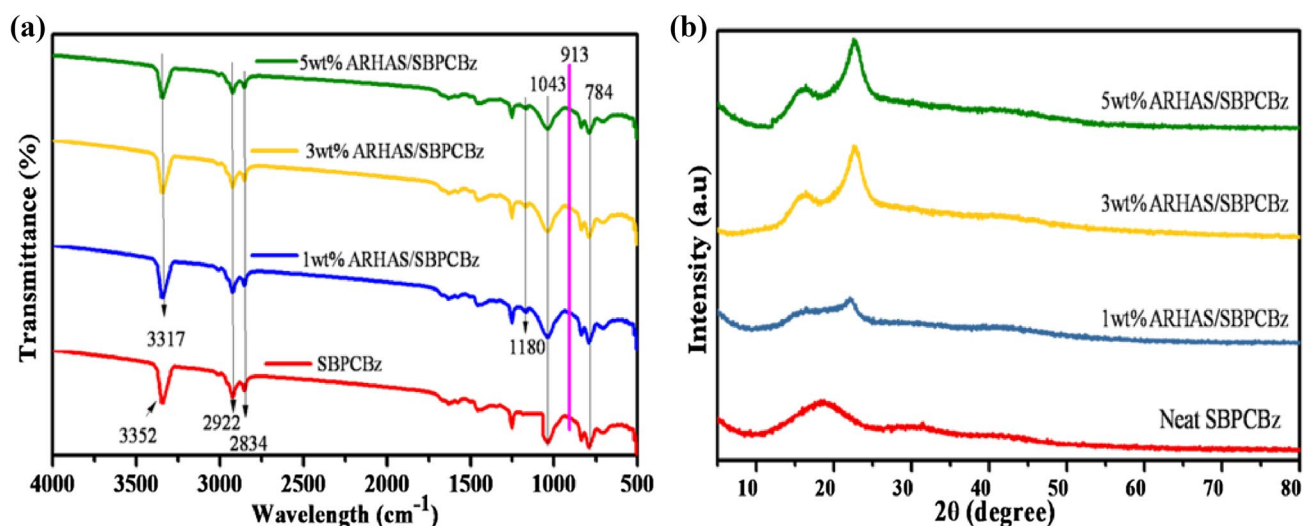


Fig. 6 **a** FTIR spectra and **b** XRD studies of SBPCBz matrix and ARHAS/SBPCBz composites

the cardanol. The disappearance of the absorption peak at 913 cm^{-1} infers the cleavage of benzoxazine ring structure during the thermal curing process. The absorption peaks obtained at 1043 and 784 cm^{-1} confirm the presence of $-\text{Si}-\text{O}-\text{Si}-$ linkage due to the reinforcement of amine functionalized natural rice husk ash silica. The peak appeared at 1180 cm^{-1} for 1, 3 and 5 wt% of ARHAS/SBPCBz hybrid composites is due to the presence of $\text{Si}-\text{O}-\text{C}$ linkage of amine functionalized rice husk ash silica, while this peak was not appearing in the case of neat SBPCBz matrices.

X-ray diffraction analyses were carried out to assess the diffraction patterns of siloxane based cardanol-benzoxazine and its composites (Fig. 6b). The broad peak at about $2\theta = 18.5^\circ$ was obtained for neat SBPCBz matrix. For varying weight percentages of ARHAS reinforced SBPCBz composites show two peaks. The stretched peak appeared at about $2\theta = 15.49^\circ$ for varying weight percentages of ARHAS in ARHAS/SBPCBz composites is due to the soft segment of siloxane based cardanolbenzoxazine matrix present in the composites. The second amorphous peaks obtained at $2\theta = 22.7^\circ$ for 1 wt% ARHAS/SBPCBz, 3 wt% ARHAS/SBPCBz and 5wt% ARHAS/SBPCBz are due to the hard segment of amine functionalized rice husk ash silica present in the composites [60].

The cured siloxane based cardanol-benzoxazine matrix and its composites reinforced with varying weight percentages of amine functionalised rice husk ash silica surface structures were predicted through the SEM (Fig. 7) and TEM (Fig. 8) studies. From Fig. 7, the flexible film of neat SBPCBz exhibits the uniform and smooth surface, while the reinforcement of amine functionalized rice husk ash silica creates the roughness on the surface of the composite films [61]. In addition, the surface roughness are getting

increased with respect to the increase in weight percentage of amine functionalized rice husk ash silica as 0, 1, 3 and 5 wt% to siloxane based polycardanolbenzoxazine. Further, the reinforcement of amine functionalised rice husk ash silica alters the chemical composition of the siloxane based cardanol-benzoxazine structure and hence, the roughness of surface were increased according to weight percentages of the reinforcement.

The TEM images of amine functionalized rice husk ash silica reinforced siloxane based cardanol-benzoxazine composites were screened at different magnifications and the images are presented in Fig. 8. The porous spots in the interior of the sample segment was noticed along with the uniform distribution of rice husk ash silica in the composite material and the uniform distribution indicates good compatibility resulted between amine functionalized rice husk ash silica and siloxane based cardanol-benzoxazine. The existence of nano-porous region was also noticed, which in turn contributes to low dielectric behaviour. Furthermore, the formation of nano-porous structure may be due to the intermolecular and intra-molecular hydrogen bonding resulted between the benzoxazine molecules during the curing of siloxane based cardanolbenzoxazine in the presence of amine functionalized rice husk ash silica.

Dielectric Properties of SBPCBz Matrix and ARHAS/SBPCBz Composites

Figure 9a presents the dielectric constant values of cured siloxane based cardanol-benzoxazine and varying weight percentages of amine functionalised rice husk ash silica reinforced composites at ambient temperature. The value of dielectric constant decreased from 2.447 to 1.617 at 1 MHz

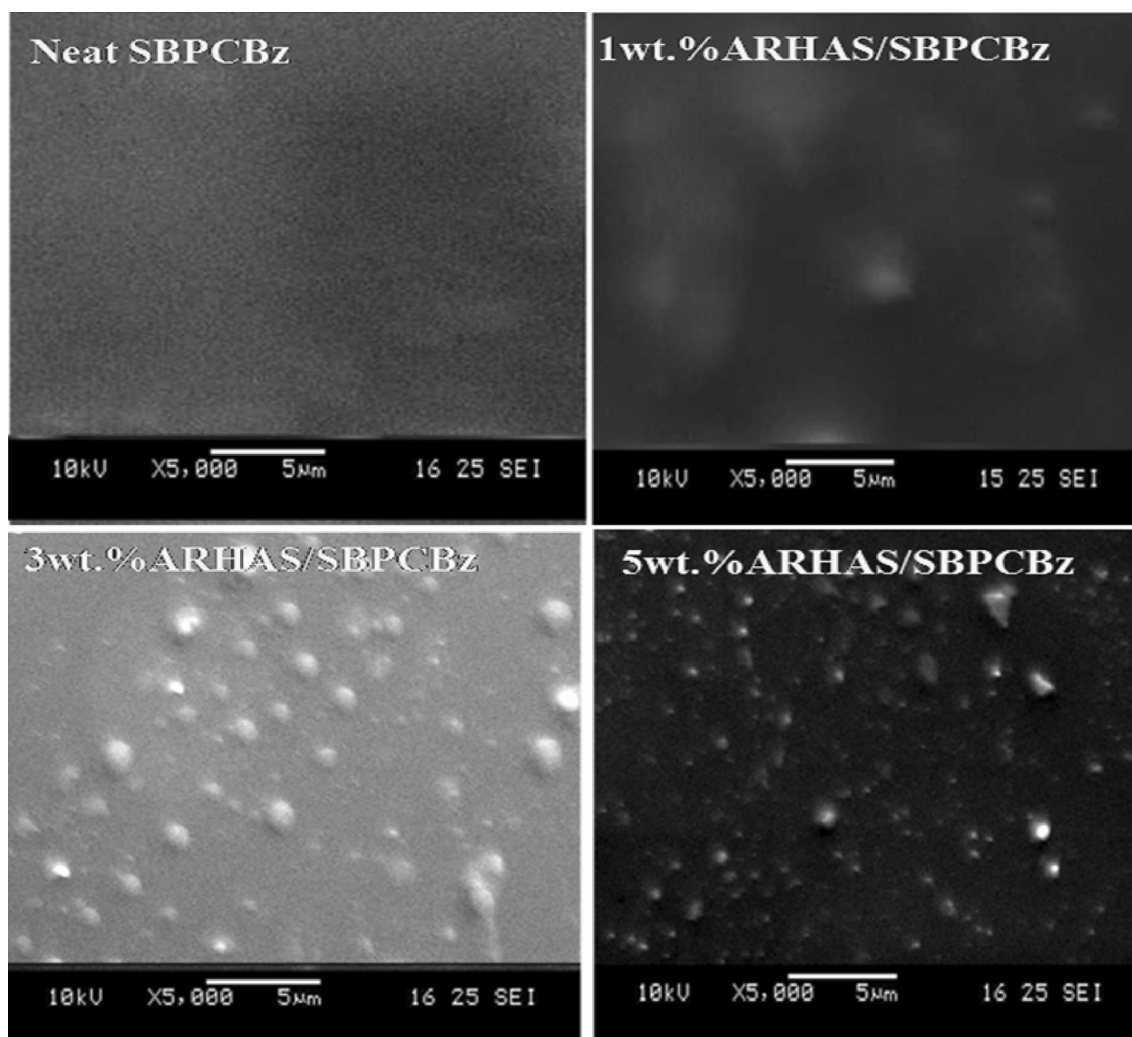


Fig. 7 SEM images of neat SBPCBz, 1 wt% ARHAS/SBPCBz, 3 wt% ARHAS/SBPCBz and 5 wt% ARHAS/SBPCBz composites

for ARHAS/SBPCBz in accordance with the concentration of ARHAS, which is due to the formation of porous structure imparted by inter- molecular and intra- molecular hydrogen bonding [62]. The significant lowering of the value of dielectric constant was contributed by the interfacial arrangement of $-\text{Si}-\text{O}-\text{Si}-$ linkage from rice husk ash silica, which in turn reduce the polarization of cardanol-benzoxazine composites.

The values of dielectric loss obtained for neat SBPCBz and varying weight percentages of (1, 3 and 5 wt%) ARHAS/SBPCBz composites are presented in Fig. 9b. The $\tan \delta$ values decreased from 0.012 to -0.005 at 1 MHz (Table 2) for neat SBPCBz to 5 wt% ARHAS/SBPCBz composite. The decrease in the value of dielectric loss is due to the moisture resistant behaviour imparted by functionalized silica reinforcement and the formation of intra-molecular hydrogen bonding from polar OH, N and restricted polarization by the amine functionalized rice husk ash silica [63].

This hydrophobic nature of the prepared polymer matrix and composite materials will not create fluctuations by passing current [64]. Thus, such a property influences to decrease the value of dielectric constant and loss, which is expected to act as an insulating material in electronic fields [65]. This also proves that there was a formation of insulating segment inside the polymeric benzoxazine nanocomposites while reinforcing with different weight percentages of amine incorporated rice husk ash silica (ARHAS) and this also leads to high thermal stability which was displayed by TGA thermograms (Fig. 10a).

Thermal Behaviour of SBPCBz Monomer, SBPCBz Matrix and ARHAS/SBPCBz Samples

Figure 10 shows the cure behaviour of siloxane modified benzoxazine obtained from DSC analysis and the resulted siloxane modified benzoxazine possesses a surprisingly low

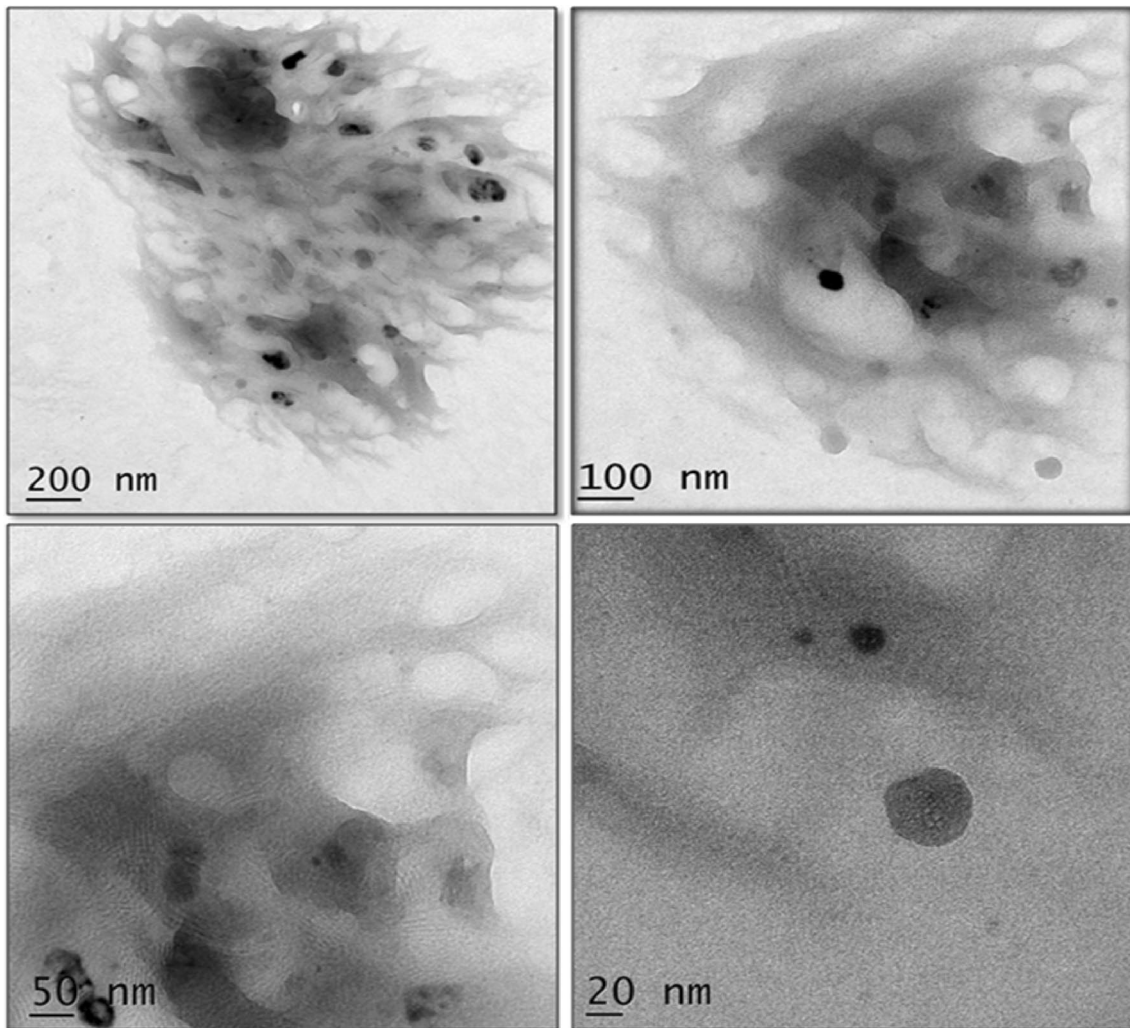


Fig. 8 TEM image of ARHAS/SBPCBz composite at different magnifications

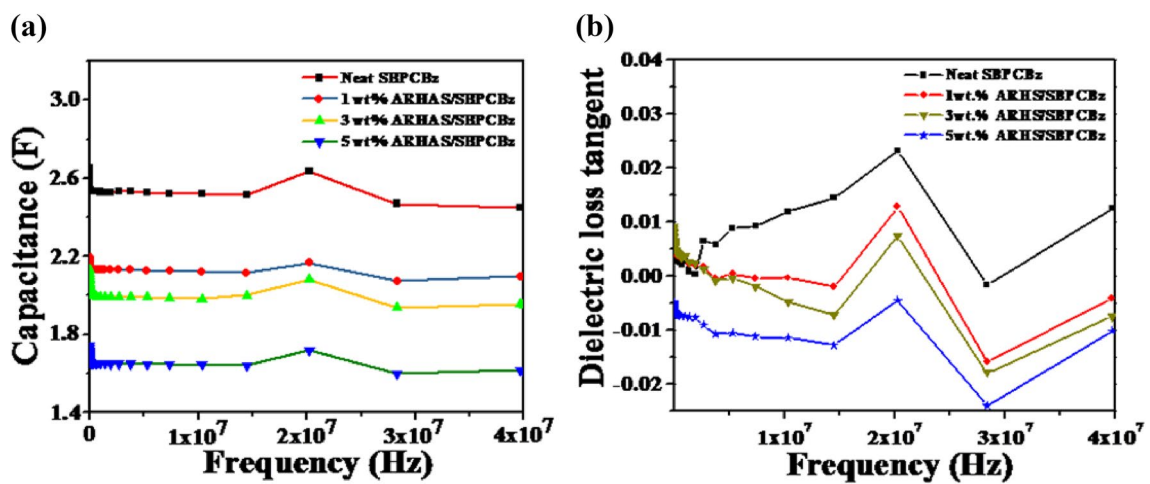
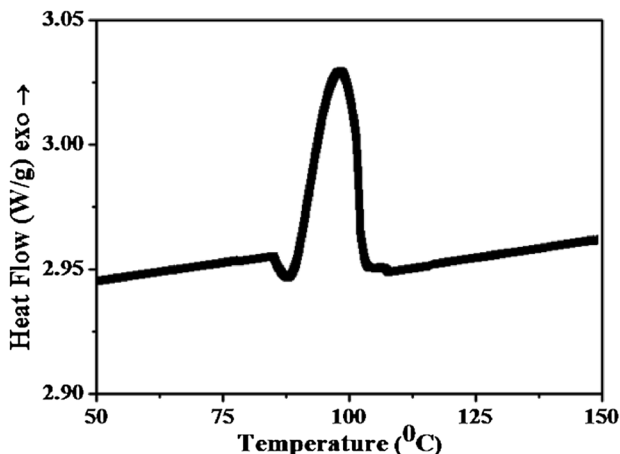


Fig. 9 a Dielectric constant and b dielectric loss curves of neat SBPCBz matrix and ARHAS/SBPCBz composites

Table 2 Thermograms and dielectric data of the siloxane based polycardanolbenzoxazine and ARHAS/SBPCBz nanocomposites

S. no	Samples	T _g (°C)	5% wt. loss (°C)	10% wt. loss (°C)	T _{max} (°C)	Char yield at 800 °C	Dielectric constant (K)	Dielectric loss
1.	Neat SBPCBz	94.07	282	319	450	17.59	2.447	0.012
2.	1 wt% ARHAS/SBPCBz	99.11	290	325	455	23.87	2.098	0.008
3.	3 wt% ARHAS/SBPCBz	103.32	297	334	457	25.89	1.957	0.006
4.	5 wt% ARHAS/SBPCBz	107.52	305	342	464	28.72	1.617	−0.005

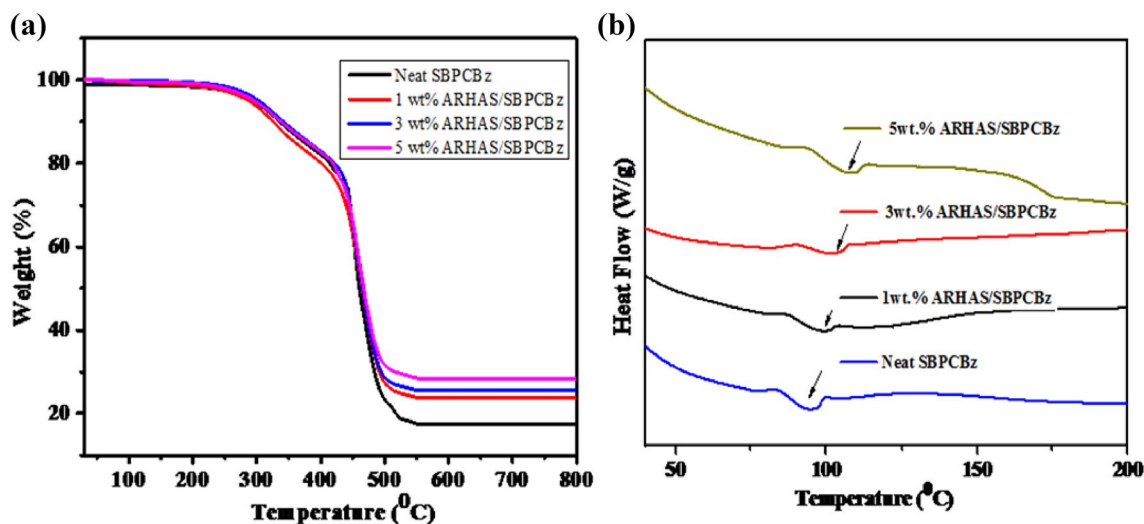
**Fig. 10** DSC curve obtained for siloxane based renewable cardanol benzoxazine monomer

cure temperature in the range of 80–110 °C when compared to that of conventional benzoxazines (220–280 °C).

The TGA data obtained for neat SBPCBz and varying weight percentages of ARHAS/SBPCBz composites are presented in Fig. 11a and Table 2. The curves presented in Fig. 11a clearly demonstrate that the thermal stability

of cured siloxane based cardanol-benzoxazine composites reinforced with varying weight percentages of amine functionalized rice husk silica possesses higher stability than that of neat polycardanolbenzoxazine. Further, it was also noticed that the thermal stability of both siloxane based cardanol-benzoxazine and amine functionalized rice husk silica reinforced hybrid composites are better than that of conventional benzoxazines due to the presence of siloxane and the existence of inter- molecular and intra -molecular hydrogen bonding [66, 67]. The value of percentages of the char yield obtained at 800 °C are 17.59, 23.87, 25.89, and 28.72 for neat SBPCBz, 1 wt% ARHAS/SBPCBz, 3 wt% ARHAS/SBPCBz and 5 wt% ARHAS/SBPCBz, respectively. The value of char yield increases with increase in weight percentage of bio-silica reinforcement, which indicates these hybrid composite materials possess high thermal stability with improved flame retardant behaviour.

From differential scanning analysis, the values of T_g for neat SBPCBz, 1 wt% ARHAS/SBPCBz, 3 wt% ARHAS/SBPCBz and 5 wt% ARHAS/SBPCBz are presented in Fig. 11b and Table 2. The T_g values were increased from 94.07 to 107.52 °C according to the percentage content of ARHAS and this may be explained due to the formation of entangled network structure as well as the presence of strong

**Fig. 11** TGA (a) and DSC (b) thermograms of neat SBPCBz and different weight percentages of ARHAS/SBPCBz composites

inter molecular hydrogen bonding, which in turn causes the restricted segmental motion in the hybrid composite systems [68].

Corrosion Resistant Studies in Sea Water

The microscopic photo images were taken at initial period (a_1, b_1, c_1, d_1), at the end of 24 h (a_2, b_2, c_2, d_2), at the end of 90 days (a_3, b_3, c_3, d_3) and at the end of 210 days (a_4, b_4, c_4, d_4) are shown in Fig. 12. The corrosion resistant behaviour in natural sea water was tested manually by using microscope available in the microbiology lab. From the microscopic photo results, it was concluded that the natural sea water did not cause any significant changes on surfaces of the SBPCBz matrix and ARHAS/SBPCBz composite materials. This makes a conclusion that the prepared polymer benzoxazine and composites are highly stable in sea water. Therefore, these results suggest that SBPCBz matrix and ARHAS/SBPCBz hybrid composites can be used an excellent coating material against bio fouling in seawater

and marine environment [69] for better performance with enhanced longevity.

Further, SEM measurements were also carried out after immersing the polymer composite films in natural sea water collected from East-Coast of Bay of Bengal, Cuddalore to ascertain the antifouling effect exhibited by them (Fig. 13). From the SEM results, it was concluded that the coatings developed using siloxane modified benzoxazine matrices and bio-silica reinforced composites show an excellent anti-fouling behaviour.

Anticorrosion Performance of SBPCBz Matrix and ARHAS/SBPCBz Composites

The semi circle Nyquist plot obtained from the mild steel and benzoxazine matrix and composites coated mild steel are shown in Fig. 14. The broad and larger semi circle in the Nyquist plots indicate the higher charge transfer resistance (R_{ct}) of the electrode/electrolyte interface and thus, the charge transfer resistance obtained are directly related

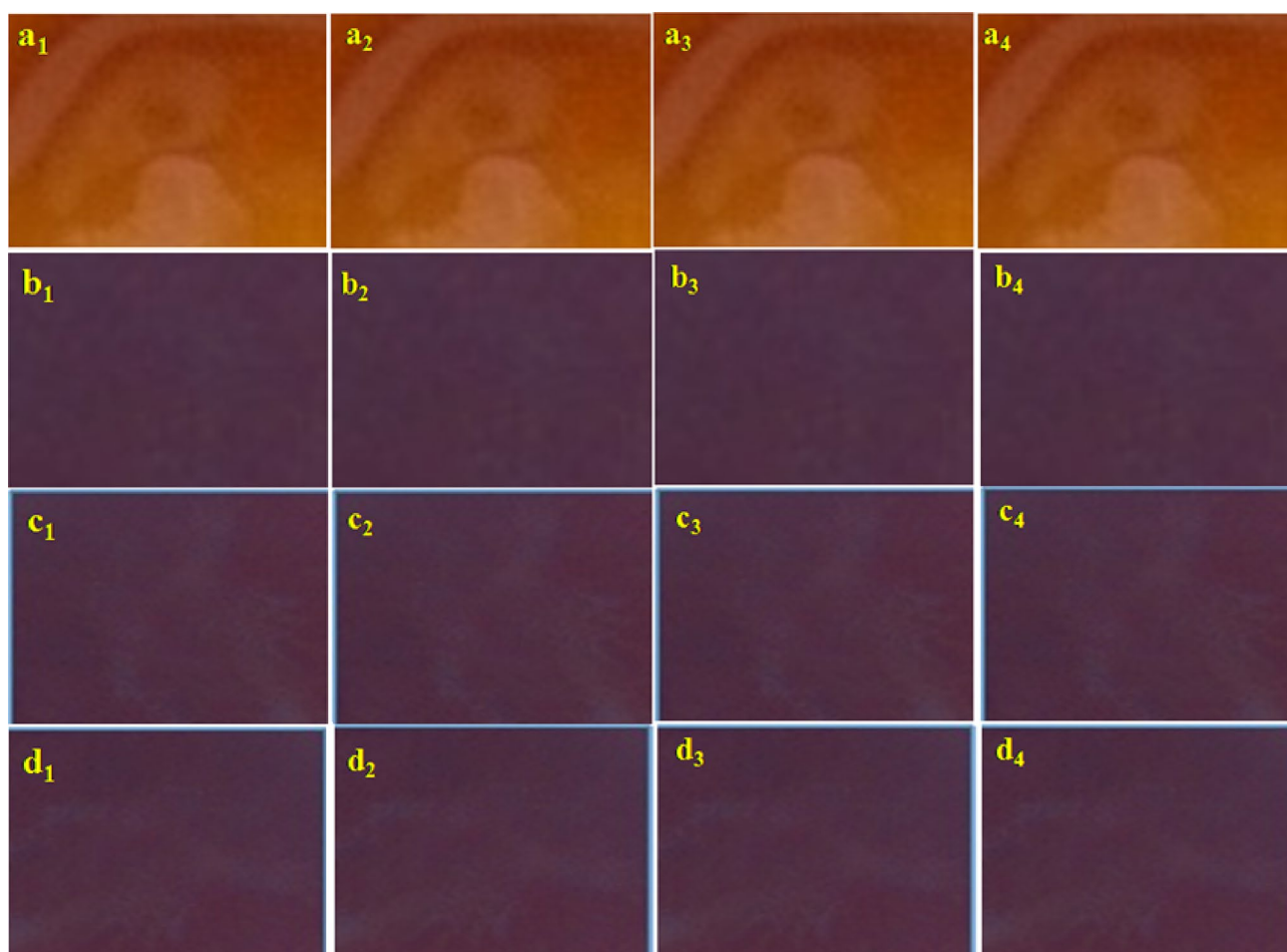


Fig. 12 Microscopy photo images of neat SBPCBz (**a**), 1 wt% ARHAS/SBPCBz (**b**), 3 wt% ARHAS/SBPCBz (**c**) and 5 wt% ARHAS/SBPCBz (**d**) films placed in the seawater at different intervals of time

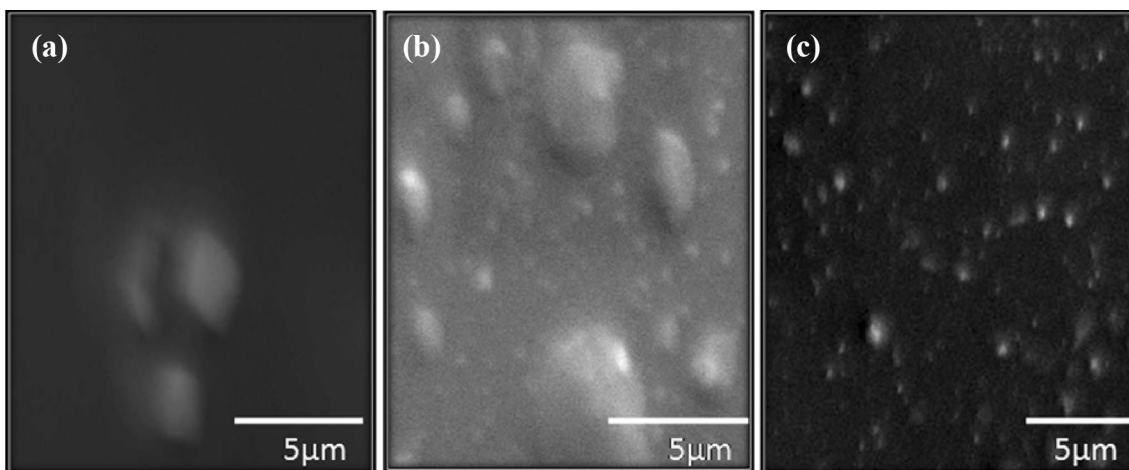


Fig. 13 SEM images of after immersing in the sea water **a** 1 wt% ARHAS/SBPCBz, **b** 3 wt% ARHAS/SBPCBz and **c** 5 wt% ARHAS/SBPCBz composites

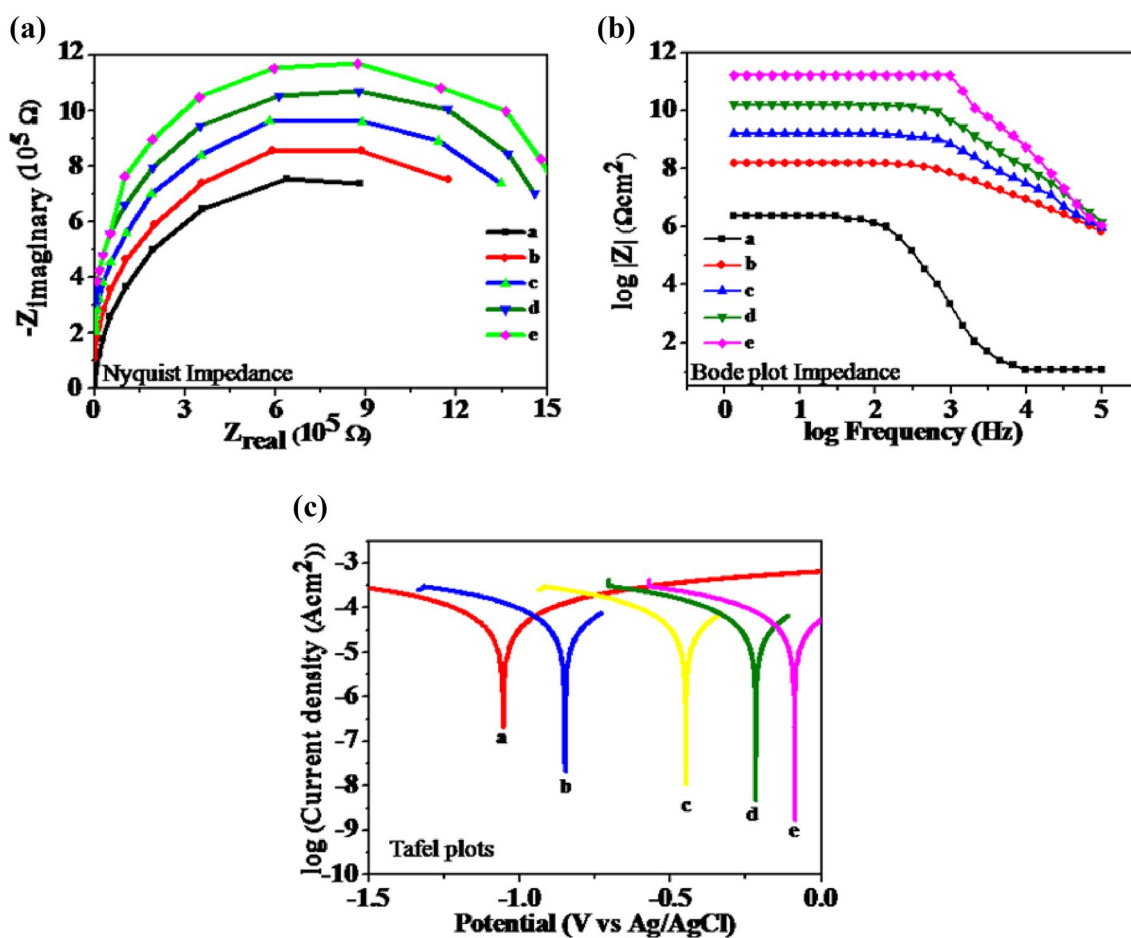


Fig. 14 Electrochemical corrosion studies for **a** bare mild steel, **b** neat SBPCBz, **c** 1 wt% ARHAS/SBPCBz, **d** 3 wt% ARHAS/SBPCBz and **e** 5 wt% ARHAS/SBPCBz composites

to the diameter of the semicircle. Accordingly, the increasing semi circle was noticed for moving from bare steel to coated steel specimens (Fig. 14) indicating the improved corrosion resistance effect offered by coated mild steel specimen when compared to that of bare mild steel. In addition, it was also noticed that the corrosion resistance increased with increasing the percentage concentration of functionalized bio-silica reinforcement, which is due to the formation of increasing effect of passive protective layer [70–72].

Bode spectrum is a plot of dimension modulus impedance $|Z|$ with respect to frequency for the uncoated and coated with benzoxazine materials in the mild steel (Fig. 14). The Bode plot gives an idea about the electrical response of the polymeric composite coatings on mild steel with respect to the log frequency. The magnitude of Bode plot impedance appeared as a straight line and decrease in impedance $|Z|$ slope was observed nearly at 90° , which indicates that the electrochemical reaction was almost absence on the surface of mild steel specimen coated with polymeric composites compared to that bare mild steel plate (Fig. 14). Hence it is concluded that the hybrid composite coatings developed in the present work function as effective barriers against corrosion property in accordance with the previous reports [73, 74].

The Tafel plots are also used to determine the corrosion resistance behaviour of uncoated steel specimen and steel specimen coated with siloxane based cardanol-benzoxazine and its composites are shown in Fig. 14. It was observed that the corrosion potentials (E_{corr}) were changed from -1.0564 to -0.0916 for neat matrix to ARHAS reinforced hybrid benzoxazine composites. The corrosion resistant (E_{corr}) potential was shifted to more positive in accordance to weight percentage of the functionalized rice husk silica. From the results, it is ascertained that the incorporation of ARHAS restricts the corrosion by changing the corrosion potential from more negative to less negative or near to zero values [75, 76]. The enhanced corrosion resistance behaviour of coated specimens may be explained due to the hydrophobic nature of bio-silica reinforcements in addition to the presence of a long chain hydrocarbon moiety [77]. Data resulted from corrosion studies suggested that the bio-silica reinforced siloxane based cardanol-benzoxazine can be used as an effective and efficient coating material to protect mild steel specimens from corrosion.

Conclusion

The siloxane based cardanol-benzoxazine synthesized was reinforced with varying weight percentages of aminosilane functionalized bio-silica derived from rice husk ash to obtain hybrid composites and their thermal stability, morphology, dielectric behaviour, and corrosion protection against mild

steel specimen surface were studied. Result obtained from differential calorimetric analysis infer that the newly developed siloxane modified cardanol-benzoxazine cures at significantly very low temperature than that of conventional benzoxazines. Further, in addition to cure behaviour, the newly developed benzoxazine with siloxane skeleton coupled with long chain cardanol skeleton will contribute to the formation of flexible film. Both the low cure temperature and flexible behaviour of siloxane modified cardanol-benzoxazine make the material suitable for high performance coating and insulation applications. Further, data obtained from thermal, morphological, dielectric and corrosion resistant studies indicate that these hybrid bio-based benzoxazine composite materials may be considered for a future use in the form of coatings, adhesives, sealants and matrices for different engineering applications in particular low k inter-layer dielectrics in microelectronics and protection of mild steel surfaces from corrosion under adverse environmental conditions.

References

- Xu G, Shi T, Xiang Y, Yuan W, Wang Q (2015) RSC Adv 5:77429–77436
- Puchot L, Verge P, Fouquet T, Vancaeyzeele C, Vidal F, Habibi Y (2016) Green Chem 18:3346–3353
- Ejfler J, Krauzy-Dziedzic K, Szafert S, Lis T, Sobota P (2009) Macromolecules 42:4008–4015
- Sharma P, Lochab B, Kumar D, Roy PK (2016) ACS Sustain Chem Eng 4:1085–1093
- Li S, Zou T, Feng L, Liu X, Tao M (2013) J Appl Polym Sci 128:4164–4171
- Mohapatra S, Golok BN (2013) Ind Eng Chem Res 52:5951–5957
- Liu X, Zhang R, Li T, Zhu P, Zhuang Q (2017) ACS Sustain Chem Eng 5:10682–10692
- Ma H-X, Li J-J, Qiu J-J, Liu Y, Liu C-M (2017) ACS Sustain Chem. Eng 5:350–359
- Calo E, Maffezzoli A, Mele G, Martina F, Selma EM, Tarzia A, Stifani C (2007) Green Chem 9:754–759
- Rao BS, Palanisamy A (2011) React Funct Polym 71:148–154
- Li S, Yan S, Yu J, Yu B (2011) J Appl Polym Sci 122:2843–2848
- Lligadas G, Tuzun A, Juan CR, Galiaa M, Cadiz V (2014) Polym Chem 5:6636–6644
- Lin CH, Cai SX, Leu TS, Hwang TY, Lee HH (2006) J Polym Sci A 44:3454–3468
- Voirin C, Caillol S, Nilakshi VS, Bhausheb VT, Boutevin B, Prakash PW (2014) Polym Chem 5:3142–3162
- Yagci Y, Kiskan B, Ghosh NN (2009) J Polym Sci A 47:5565–5576
- Nguyen TKL, Livi S, Bluma GS, Guilherme MOB, Gerard J-F, Duchet-Rumeau J (2017) ACS Sustain Chem Eng 5:8429–8438
- Chen J, Nie X, Liu Z, Mi Z, Zhou Y (2015) ACS Sustain Chem Eng 3:1164–1171
- Y. Gu, Q.-C. Ran, *Handbook of Benzoxazine Resins*, Chapter 28 (2011), pp. 481–494
- Rimdisit S, Kunopast P, Dueramae I (2011) Polym Eng Sci 51:1797–1807
- Bo C, Hu L, Chen Y, Yang X, Zhang M, Zhou Y (2018) J Mater Sci 53:10784–10797

21. Agag T, An SY, Ishida H (2013) *J Appl Polym Sci* 127:2710–2714
22. Breslin CB, Fenelon AM, Conroy KG (2005) *Mater Des* 26:233–237
23. Zhou C, Lin J, Lu X, Xin Z (2016) *RSC Adv* 6:28428–28434
24. Renaud A, Poorteman M, Escobar J, Dumas L, Paint Y, Bonnaud L, Dubois P, Olivier M-G (2017) *Prog Org Coat* 112:278–287
25. Deepak MP, Ganesh AP, Mhaske ST (2017) *Prog Org Coat* 105:18–28
26. Zhou C, Lu X, Xin Z, Liu J (2013) *Corros Sci* 70:145–151
27. Shukla S, Mahata A, Pathak B, Lochab B (2015) *RSC Adv* 5:78071–78080
28. Sini NK, Bijwe J, Indra KV (2014) *J Polym Sci A* 52:7–11
29. Yang D, Du B, Yan Y, Li H, Zhang D, Fan T (2014) *ACS Appl Mater Interfaces* 6:2377–2385
30. Zhang Y, Zheng R, Zhao J, Ma F, Zhang Y, Meng Q (2014) *Biomed Res Int* 2014:496878–496885
31. Malek F, Cheng EM, Nadiyah O, Nornikman H, Ahmed M, Abdaziz MZA, Osman AR, Soh PJ, Azremi AAH, Hasnain A, Taib MN (2011) *Prog Electromagn Res* 117:449–477
32. Ndazi BS, Karlsson S, Tesha JV, Nyahumwa CW (2007) *Composites A* 38:925–935
33. Demirbas A (2004) *Prog Energy Combust Sci* 30:219–230
34. Kamisah MM, Siti Munirah H, Mansor MS (2007) *Ionics* 13:223–225
35. Thalita SG, Simone N, Goncalves M, Flavia CAF, Mandelli D, Wagner AC (2013) *ACS Sustain Chem Eng* 1:1381–1389
36. Chen K-T, Wang J-X, Dai Y-M, Wang P-H, Liou C-Y, Nien C-W, Wu J-S, Chen C-C (2013) *J Taiwan Inst Chem Eng* 44:622–629
37. Kanimozhi K, Sethuraman K, Selvaraj V, Alagar M (2014) *Front Chem* 2:1–9
38. Calo E, Maffezzoli A, Mele G, Martina F, Mazzetto SE, Tarzia A, Stifani C (2007) *Green Chem* 9:754–759
39. Amarnath N, Appavoo D, Lochab B (2018) *ACS Sustain Chem Eng* 6:389–402
40. Selvaraj V, Jayanthi KP, Lakshmikandhan T, Alagar M (2015) *RSC Adv* 5:48898–48907
41. Krishnadevi K, Selvaraj V (2015) *New J Chem* 39:6555–6567
42. Prasanna D, Selvaraj V (2016) *Korean J Chem Eng* 33:1489–1499
43. Stober W, Fink A, Bohn E (1968) *J Colloid Interface Sci* 26:62–69
44. Abadikhah H, Kalali EN, Behzadi S, Khan SA, Xu X, Agathopoulos S (2018) *Polymer* 154:200–209
45. Jing M, Fu Y, Fei X, Tian J, Zhi H, Zhang H, Xu L, Wang X, Wang Y (2017) *Poly Chem* 8:35553–35559
46. Bonhomme S, Cuer A, Delort AM, Lemaire J, Sancelme M, Scott G (2003) *Polym Degrad Stab* 81:441–452
47. Li S, Zhao C, Gou H, Li H, Li Y, Xiang D (2017) *RSC Adv* 7:55796–55806
48. Lochab B, Indra KV, Bijwe J (2010) *J Therm Anal Calorim* 102:769–774
49. Han L, Iguchi D, Phwey SG, Heyl T, Victoria MS, Carlos RA, Ohashi S, Daniel JL, Ishida H (2017) *J Phys Chem A* 121:6269–6282
50. Puchot L, Verge P, Fouquet T, Vancaeyzeele C, Vidal F, Habibi Y (2016) *Green Chem* 18:3346–3353
51. Wu J-Y, Mohamed MG, Kuo S-W (2017) *Polym Chem* 8:5481–5489
52. Rao BS (2013) *A Palanisamy. Eur Polym J* 49:2365–2376
53. Li C, Zuo C, Fan H, Yu M, Li B (2012) *Thermochim Acta* 545:75–81
54. Huh P, Kim B-S, Kim S-C (2012) *Thin Solid Films* 520:5557–5560
55. Lochab B, Shukla S, Varma IK (2014) *RSC Adv* 4:21712–21752
56. Brassard J-D, Sarkar DK, Perron J (2012) *Appl Sci* 2:453–464
57. Zhang L, Zhu Y, Li D, Wang M, Chen H, Wu J (2015) *RSC Adv* 5:96879–96887
58. Kolahdoozan M, Mirsafaei R (2012) *Des Monomers Polym* 15:289–301
59. Wang J, Fang X, Wu MQ, He XY, Liu WB, Shen XD (2011) *Eur Polym J* 47:2158–2168
60. Ivan SS, Spirikova M, Ostojic S, Stefanov P, Vladimir BP, Marija VP (2017) *Appl Clay Sci* 149:136–146
61. John PH, Aoife D, Michael AM, Justin DH (2007) *J Mater Chem* 17:3881–3887
62. Hariharan A, Srinivasan K, Murthy C, Alagar M (2018) *New J Chem* 42:4067–4080
63. H. Ishida, T. Agag, *Handbook of Benzoxazine Resins* (Elsevier B.V., 2011). ISBN: 978-0-444-53790-4
64. Krishnadevi K, Selvaraj V (2016) *High Perform Polym* 28:1–14
65. Pourrahimi AM, Pallon LKH, Liu D, Hoang TA, Gubanski S, Hedenqvist MS, Olsson RT, Gedde UW (2016) *ACS Appl Mater Interfaces* 8:14824–14835
66. H Ishida, P Froimowicz, *Advanced and Emerging Polybenzoxazine Science and Technology* (Elsevier, eBook, 2017). ISBN: 9780128041857
67. Ates S, Dizman C, Aydogan B, Kiskan B, Torun L, Yagci Y (2011) *Polymer* 52:1504–1509
68. Hu W-H, Huang K-W, Kuo S-W (2012) *Polym. Chem* 3:1546–1554
69. Caldona EB, De Leon AC, Thomas PG, Naylor DF III, Pajarito BB, Advincula RC (2017) *Ind Eng Chem Res* 56:1485–1497
70. Selvaraj V, Rhagavarshini TR, Krishnadevi K (2018) *Polym Bull* 76:469–494
71. Zhou C, Lu X, Xin Z, Liu J, Zhang Y (2014) *Corros Sci* 80:269–275
72. Mouanga M, Bercot P (2010) *Corros Sci* 52:3993–4000
73. Zhang W, Li L, Yao S, Zheng G (2007) *Corros Sci* 49:654–661
74. Metikos Hukovic M, Kalcec ET, Kwokal A, Piljac J (2003) *Surf Coat Technol* 165:40–50
75. Taleb HI, Zour MA (2011) *Int J Electrochem Sci* 6:6442–6455
76. Eugene BC, de Leon AC, Bryan BP, Rigoberto CA (2017) *Appl Surf Sci* 422:162–171
77. Eugene BC, de Leon AC, Joey DM, Kramer Joseph AL, Bryan BP, Rigoberto CA (2018) *React Funct Polym* 123:10–19

Publisher's Note Springer Nature remains neutral with regard to jurisdictional claims in published maps and institutional affiliations.